OPEN

Relating Molecular T Cell–mediated Rejection Activity in Kidney Transplant Biopsies to Time and to Histologic Tubulitis and Atrophy-fibrosis

Katelynn S. Madill-Thomsen, PhD,[1] Georg A. Böhmig, MD,[2] Jonathan Bromberg, MD, PhD,[3] Gunilla Einecke, MD, PhD,[4] Farsad Eskandary, MD, PhD,[2] Gaurav Gupta, MD,[5] Marek Myslak, MD, PhD,[6] Ondrej Viklicky, MD, PhD,[7] Agnieszka Perkowska-Ptasinska, MD, PhD,[8] Kim Solez, MD,[9] Philip F. Halloran, MD, PhD,[1,10] and the INTERCOMEX Investigators*

Background. We studied the variation in molecular T cell–mediated rejection (TCMR) activity in kidney transplant indication biopsies and its relationship with histologic lesions (particularly tubulitis and atrophy-fibrosis) and time posttransplant. **Methods.** We examined 175 kidney transplant biopsies with molecular TCMR as defined by archetypal analysis in the INTERCOMEX study (ClinicalTrials.gov #NCT01299168). TCMR activity was defined by a molecular classifier. **Results.** Archetypal analysis identified 2 TCMR classes, TCMR1 and TCMR2: TCMR1 had higher TCMR activity and more antibody-mediated rejection ("mixed") activity and arteritis but little hyalinosis, whereas TCMR2 had less TCMR activity but more atrophy-fibrosis. TCMR1 and TCMR2 had similar levels of molecular injury and tubulitis. Both TCMR1 and TCMR2 biopsies were uncommon after 2 y posttransplant and were rare after 10 y, particularly TCMR1. Within late TCMR biopsies, TCMR classifier activity and activity molecules such as *IFNG* fell progressively with time, but tubulitis and molecular injury were sustained. Atrophy-fibrosis was increased in TCMR biopsies, even in the first year posttransplant, and rose with time posttransplant. TCMR1 and TCMR2 both reduced graft survival, but in random forests, the strongest determinant of survival after biopsies with TCMR was molecular injury, not TCMR activity. **Conclusions.** TCMR varies in intensity but is always strongly related to molecular injury and atrophy-fibrosis, which ultimately explains its effect on survival. We hypothesize, based on the reciprocal relationship with hyalinosis, that the TCMR1-TCMR2 gradient reflects calcineurin inhibitor drug underexposure, whereas the time-dependent decline in TCMR activity and frequency after the first year reflects T-cell exhaustion.

(*Transplantation* 2023;107: 1102–1114).

Received 30 June 2022. Revision received 29 August 2022.

Accepted 12 September 2022.

[1] *Alberta Transplant Applied Genomics Centre, Edmonton, AB, Canada.*

[2] *Division of Nephrology and Dialysis, Department of Medicine III, Medical University of Vienna, Vienna, Austria.*

[3] *Department of Surgery, University of Maryland, Baltimore, MD.*

[4] *Department of Nephrology, Hannover Medical School, Hannover, Germany.*

[5] *Division of Nephrology, Virginia Commonwealth University, Richmond, VA.*

[6] *Department of Clinical Interventions, Department of Nephrology and Kidney Transplantation SPWSZ Hospital, Pomeranian Medical University, Szczecin, Poland.*

[7] *Department of Nephrology and Transplant Center, Institute for Clinical and Experimental Medicine, Prague, Czech Republic.*

[8] *Department of Pathology, Medical University of Warsaw, Warsaw, Poland.*

[9] *Department of Laboratory Medicine and Pathology, Division of Anatomical Pathology, University of Alberta, Edmonton, Canada.*

[10] *Division of Nephrology and Transplant Immunology, Department of Medicine, University of Alberta, Edmonton, AB, Canada.*

**A full list of INTERCOMEX Investigators is included in Table S1 (SDC, http://links.lww.com/TP/C603).*

P.F.H. holds shares in Transcriptome Sciences Inc (TSI), a University of Alberta research company dedicated to developing molecular diagnostics, and is supported in part by a licensing agreement between TSI and Thermo Fisher and by a research grant from Natera. P.F.H. is a consultant to Natera. The other authors declare no conflicts of interest.

This research has been supported at times by grants from Genome Canada, Canada Foundation for Innovation, the University of Alberta Hospital Foundation, the Alberta Ministry of Advanced Education and Technology, the Mendez National Institute of Transplantation Foundation, and Industrial Research Assistance Program. Partial support was also provided by funding from a licensing agreement with the One Lambda division of Thermo Fisher. P.F.H. held a Canada Research Chair in Transplant Immunology until 2008 and currently holds the Muttart Chair in Clinical Immunology.

K.S.M-T. edited and reviewed the article and was responsible for data analysis and interpretation. G.A.B., J.B., G.E., F.E., G.G., M.M., O.V., and A.P-P. contributed biopsies and edited and reviewed the article. K.S. edited and reviewed the article. P.F.H. was the principal investigator, edited and reviewed the article, and was responsible for data interpretation and study design.

CEL files are available on the Gene Expression Omnibus website (GSE124203).

Supplemental digital content (SDC) is available for this article. Direct URL citations appear in the printed text, and links to the digital files are provided in the HTML text of this article on the journal's Web site (www.transplantjournal.com).

Correspondence: Philip F. Halloran, MD, PhD, Alberta Transplant Applied Genomics Centre, #250 Heritage Medical Research Centre, University of Alberta, Edmonton, AB T6G 2S2, Canada. (phallora@ualberta.ca).

Copyright © 2022 The Author(s). Published by Wolters Kluwer Health, Inc. This is an open-access article distributed under the terms of the Creative Commons Attribution-Non Commercial-No Derivatives License 4.0 (CCBY-NC-ND), where it is permissible to download and share the work provided it is properly cited. The work cannot be changed in any way or used commercially without permission from the journal.

ISSN: 0041-1337/20/1075-1102

DOI: 10.1097/TP.0000000000004396

© 2022 The Author(s). Published by Wolters Kluwer Health, Inc.

INTRODUCTION

T cell–mediated rejection (TCMR) is the fundamental reaction of the mammalian host to allogeneic tissue and was the principal barrier to successful organ transplantation before effective immunosuppressive drugs (ISDs) were available. Biopsy-proven TCMR was used as the endpoint for the development of ISDs[1] and substantially decreased in frequency with the introduction of calcineurin inhibitor (CNI)/mycophenolate-based protocols,[2] leaving the main rejection phenotype as antibody-mediated rejection (AMR).[3] Nevertheless, TCMR continues to be diagnosed in approximately 10% of indication biopsies,[4] and histologic TCMR-related changes negatively impact survival.[5,6] TCMR often reflects underimmunosuppression: nonadherence,[7] ISD "minimization,"[8] or dose reduction during infections such as BK nephropathy (BKN). BKN often develops a TCMR-like process as ISD minimization continues, directed at alloantigens, BK antigens, or both.[9] Hyalinosis of the glomerular afferent arteriole, a marker for CNI exposure, is less than expected in TCMR biopsies, consistent with underimmunosuppression as a risk for TCMR.[10,11] Although TCMR becomes uncommon after 5 to 10 y, unlike AMR,[12] late TCMR (usually defined as after 1 y posttransplant) is associated with worse outcomes.[13,14]

Histologic diagnosis of TCMR largely depends on tubulitis (t-lesions) and interstitial inflammation (i-lesions). Pollak[15] described tubulitis in the native kidney in 1975 as the invasion of tubules by mononuclear cells, usually accompanied by interstitial inflammation. Sibley et al[16] in 1983 and Verani et al[17] in 1984 described tubulitis in the transplanted kidney. In 1985, Solez et al[18] recognized that the mononuclear cells in tubulitis lie between or beneath tubular epithelial cells inside the tubular basement membrane. Tubulitis was a major feature of the Banff classification in 1993[19] and remains the key histologic lesion in TCMR. Intimal arteritis (v-lesion) is less common and can be caused by TCMR, AMR, or injury.[20]

The present analysis aimed to study the variation in TCMR incidence, molecular activity, and histologic features with time posttransplant and the relative impact of these features on graft survival. We defined TCMR molecularly to permit us to assess its relationship with the diagnostic histologic lesions, particularly tubulitis. We characterized molecular TCMR using genome-wide microarray measurements interpreted by the Molecular Microscope Diagnostic System (MMDx) algorithms.[21,22] Archetypal analysis (AA) recognized 2 TCMR classes[21,22]: TCMR1 and TCMR2. TCMR1 was formerly called "mixed" but was renamed TCMR1 because some TCMR1 biopsies lack AMR activity. We defined TCMR activity by the molecular TCMR classifier[23] and its associated molecules such as *IFNG* and *LAG3*.[24]

MATERIALS AND METHODS

Study Population

We studied 1679 prospectively collected indication biopsies obtained with consent from 19 established centers under local institutional review board–approved protocols (ClinicalTrials.gov #NCT01299168; **Table S1**, **SDC**, http://links.lww.com/TP/C603). The population was previously described[22,25-27] and is summarized in **Table S2** (**SDC**, http://links.lww.com/TP/C603). Histologic diagnoses were assigned by the local pathologist following standard-of-care (SOC) Banff guidelines per study protocol. Donor-specific antibody (DSA) assessment was assigned per local SOC. The research plan for these analyses is shown in Figure 1.

Rederiving Molecular Features of Rejection

All algorithms previously derived in the 1208 biopsies[21] were updated as recently published,[22] using AA to assign 6 rejection archetype scores to each biopsy in the 1679 population, with 228 death-censored graft failures within 3 y postbiopsy. We used the scores assigned by an ensemble of 7 rejection classifiers to visualize the rejection states in principal component analysis (PCA) and assign AA groups.[21,22,28] All classifier algorithms were previously developed, trained, and tested on class comparisons comparing an abnormal condition with a more normal condition. The rejection classifiers were those predicting histologic diagnoses of AMR (AMR_{Prob}) or TCMR ($TCMR_{Prob}$) or histologic lesions ptc ($ptc>0_{Prob}$), g ($g>0_{Prob}$), cg ($cg>0_{Prob}$), i ($i>1_{Prob}$), and t ($t>1_{Prob}$).

This report focuses on the 175 biopsies in the 2 TCMR-related archetype groups, TCMR1 and TCMR2, compared with the no rejection (NR) group, and the relationships between molecular TCMR disease activity, time posttransplant, and histologic lesions. TCMR disease activity was defined as the TCMR molecular classifier score and associated transcript expression.

Principal Component Analysis

PCA was used to visualize the rejection states using classifier algorithms previously described.[21,22] PCA was therefore based on a 1679 (samples) × 7 (variables) data matrix, using the "PCA" function in the R "FactoMineR" package.[29]

Transcript Sets

Details regarding transcript sets used in these analyses are shown in **Table S3** (**SDC**, http://links.lww.com/TP/C603). Transcript sets were used as input in some analyses and to interpret results.

Statistical Analyses

All *t* tests for differential gene expression were performed using the "wilcox.test" function in base R.[30]

Survival Analyses

Survival analyses compared select biopsy subpopulations, that is, different archetypally assigned or histology classes. These analyses were done using 1 randomly selected biopsy per patient (N = 1153) and the "survfit" function from the "survival" package in R.[31]

Time Course of Archetypal Biopsy Assignment

Splines were used to show nonlinear relationships between variables. Three "knots" were selected for splines in this article, and smooth curves fit based on within-knot data with constraints so that curves between segments were joined. Overfitting was avoided by restricted cubic splines using only linear trend lines for the segments beyond the left-most and right-most knots, thereby reducing the influence of the extreme ends of these distributions where fewer

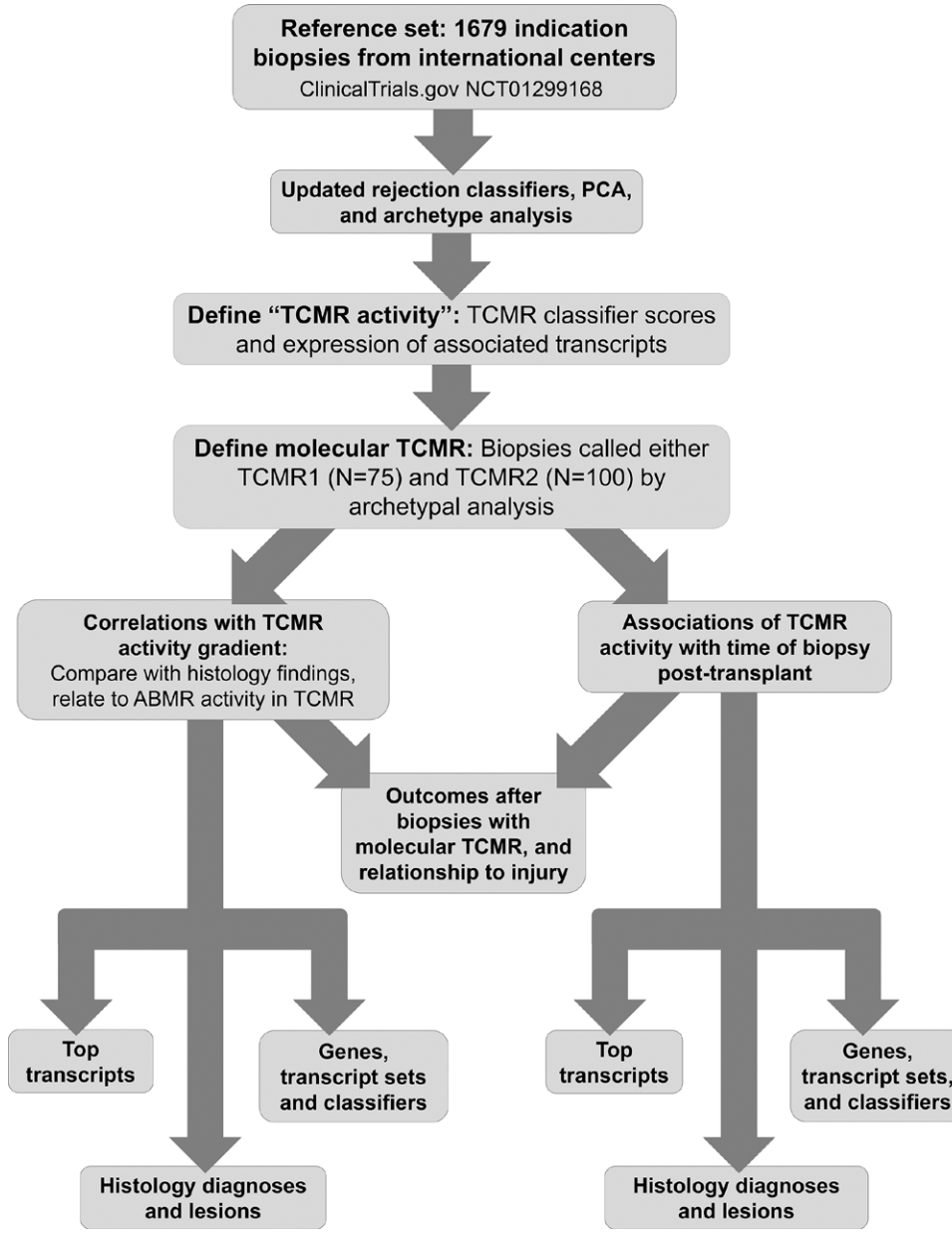

FIGURE 1. Research plan. AMR, antibody-mediated rejection; PCA, principal component analysis; TCMR, T cell–mediated rejection.

data points are available. Splines were generated using the R package "rms."[32]

Diagnoses

The dominant molecular diagnosis in each biopsy was assigned by its highest rejection archetype score: NR, TCMR1, TCMR2, early AMR (EAMR), fully developed AMR (FAMR), and late-stage AMR (LAMR). In addition, all MMDx report results are signed out by an expert to recognize additional details beyond the dominant diagnosis. All molecular diagnoses were assigned with no knowledge of local histologic findings, DSA, and C4d results. SOC histologic findings were also recorded by the local centers.

RESULTS

Patient Population

We defined TCMR molecularly to establish its relationship with various histologic features, particularly tubulitis, atrophy-fibrosis, and hyalinosis. The present analysis focuses on biopsies assigned to the TCMR1 and TCMR2 archetype groups, that is, whose dominant molecular phenotype was TCMR objectively assigned by AA. This included some biopsies that also had some AMR-related disease activity in TCMR2 (eg, mixed rejection). Note that TCMR1 and TCMR2 are archetype-assigned clusters that designate the *dominant* phenotype of the biopsy, but they both can include elements of a second rejection phenotype—AMR. We recognize this complexity in the MMDx diagnoses, where we distinguish "TCMR" from "mixed," that is, biopsies that have molecular TCMR and molecular AMR classifier scores.

Table 1 presents the molecular report signouts and histology diagnoses in all 175 archetypal TCMR1/2 biopsies. MMDx report signouts called 57 mixed (TCMR1 = 44 and TCMR2 = 13). Histology called 26 mixed (TCMR1 = 18 and TCMR2 = 8). DSA was increased in the TCMR with mixed features but was

TABLE 1.

Histologic and MMDx diagnoses and DSA in the TCMR1 vs TCMR2 biopsy groups in the 175 TCMR cohort

			Rejection archetype group		
		All TCMR (N = 175)	TCMR1 (N = 75)	TCMR2 (N = 100)	*P* TCMR1 vs TCMR2
MMDx signout diagnoses					
Rejection-related	AMR	5 (3%)	0	5 (5%)	0.07
	Possible AMR	0	0	0	1.00
	Mixed	57 (33%)	44 (59%)	13 (13%)	**<0.0001**
	TCMR	103 (59%)	31 (41%)	72 (72%)	**<0.0001**
	Possible TCMR	10 (6%)	0	10 (10%)	**0.005**
No rejection		0	0	0	1.00
Histology diagnoses					
Rejection-related	AMR	8 (5%)	4 (5%)	4 (4%)	0.73
	Transplant glomerulopathy	3 (2%)	0	3 (3%)	0.26
	AMR suspected	2 (1%)	1 (1%)	1 (1%)	1.00
	Mixed	26 (15%)	18 (24%)	8 (8%)	**0.003**
	TCMR	73 (42%)	39 (52%)	34 (34%)	**0.02**
	TCMR/BK	3 (2%)	2 (3%)	1 (1%)	0.61
	Borderline rejection	12 (7%)	2 (3%)	10 (10%)	0.07
No rejection	BK nephropathy virus	24 (14%)	3 (4%)	21 (21%)	**0.001**
	No major abnormalities	4 (2%)	1 (1%)	3 (3%)	0.64
	Others[a]	20 (11%)	5 (7%)	15 (15%)	0.09
DSA status					
		N in all TCMR (% of N = 142 tested)	N in TCMR1 (% of N = 59 tested)	N in TCMR2 (% of N = 83 tested)	*P* TCMR1 vs TCMR2
DSA positive		51 (36%)	24 (41%)	27 (33%)	0.32
DSA negative		91 (64%)	35 (59%)	56 (67%)	
DSA missing/unknown		33	16	17	

[a]Others includes diabetic nephropathy, glomerulonephritis, fibrosis and atrophy (IFTA), calcineurin inhibitor toxicity, C4d deposition without morphologic evidence for active rejection, donor origin vascular disease, pyelonephritis, systemic infection/diarrhea, and bacterial infection.
Chi-square was performed on the comparison of TCMR1 vs TCMR2 for each histologic diagnosis.
Bold values indicate significant difference between TCMR1 and TCMR2.
AMR, antibody-mediated rejection; DSA, donor-specific antibody; MMDx, Molecular Microscope Diagnostic System; TCMR, T cell–mediated rejection.

often absent, like AMR generally.[22] Details of the AMR groups were reported previously.[22] Archetype assignments recognize the dominant rejection state of the biopsy automatically assigned by highest score. Molecular report signouts often recognize additional details in archetype assignments because they consider both archetype scores and binary classifiers (**Table S4, SDC**, http://links.lww.com/TP/C603).

TCMR Archetypes in the 1679 Biopsy Population

Figure 2A and B shows the biopsy distribution colored by the 1679 archetype group assignment.[22] Principal component 1 (PC1) separated NR from all rejections, whereas principal component 2 (PC2) separated TCMR from AMR (Figure 2A). TCMR1 biopsies had slightly more negative PC2 scores than TCMR2 biopsies, reflecting rejection intensity. Principal component 3 (PC3) defined the stages of AMR (Figure 2B).

Within archetypal TCMR1/2 biopsies, the molecular AMR_{Prob} classifier scores (*y*-axis) rose as the $TCMR_{Prob}$ classifier scores rose (*x*-axis, Spearman correlation = 0.35, *P* = 1.8E–6, Figure 2C). Thus, within biopsies with molecular TCMR, the intensity of TCMR activity (the classifier score) correlates with the probability of accompanying AMR activity.

The Gradient in TCMR-related Disease Activity Within the 175 TCMR1/2 Biopsies

The scores for histologic and molecular features are outlined in Table 2 for biopsies with TCMR1, TCMR2, and biopsies with NR as a comparator. Compared with TCMR2, TCMR1 had more molecular TCMR activity (ie, increased TCMR-related classifier scores), more frequent AMR histology lesions (g- and ptc-lesions), and increased molecular AMR classifier scores. TCMR1 had very little hyalinosis, compared with TCMR2 or NR biopsies. TCMR2 had more atrophy-fibrosis, more fibrous intimal thickening (cv), and more arteriolar hyalinosis (ah). However, even in TCMR2 biopsies, hyalinosis was less than in biopsies with NR. Despite their differences, TCMR1 and TCMR2 had similar levels of tubulitis, interstitial infiltrate, and molecular injury (eg, Injury repair response-associated transcripts scores), all of which were elevated compared with NR biopsies.

Effects of Time Posttransplant on the Frequency of Molecular TCMR Within 1679 Biopsies

Consistent with previous findings,[12] the frequency of biopsies assigned to TCMR1 and TCMR2 archetypes rose after 60 d, plateaued for about 3 y, then both declined to very low levels after 10 y (Figure 3A and Table 3). The

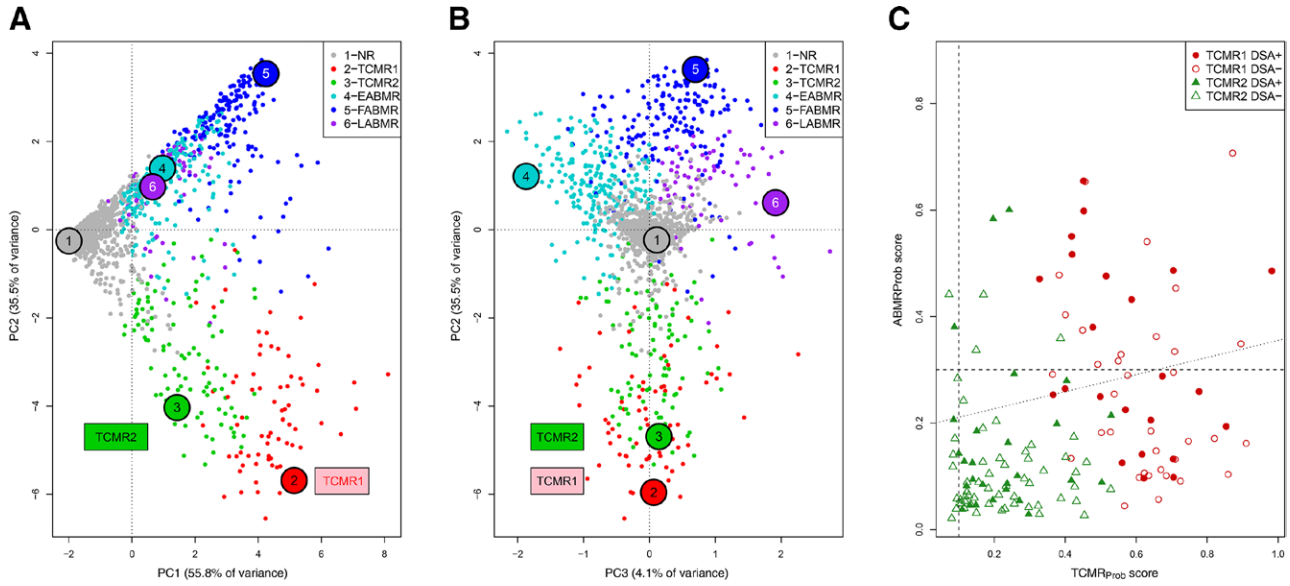

FIGURE 2. Visualizing TCMR1 and TCMR2 archetypal groups. The 1679 biopsies are shown distributed by their rejection classifiers scores in PCA and colored by their archetype assignment, with *y*-axis PC2 and *x*-axis (A) PC1, and (B) PC3. A, TCMR1 and TCMR2 show a gradient across PC1, and TCMR1 is lower than TCMR2 in PC2. B, PC3 separates AMR stages but does not separate TCMR1 and TCMR2. C, TCMR1 and TCMR2 biopsies distributed by their AMR activity (*y*-axis, AMR_{Prob} classifier scores) vs their TCMR activity (*x*-axis, $TCMR_{Prob}$ classifier scores). AMR activity was correlated with TCMR activity (Spearman correlation coefficient = 0.35, $P = 1.8E{-}6$). The biopsies from DSA-positive patients are indicated. AMR, antibody-mediated rejection; AMR_{Prob}, AMR-probability classifier; EAMR, early-stage molecular AMR; FAMR, fully developed molecular AMR; LAMR, late-stage molecular AMR; NR, no rejection; PC1, principal component 1; PC2, principal component 2; PC3, principal component 3; PCA, principal component analysis; TCMR, T cell–mediated rejection; $TCMR_{Prob}$, TCMR-probability classifier.

TABLE 2.

Differences between TCMR1 and TCMR2 in 25 scores for histology lesions and molecular scores

		No rejection (N = 1040)	TCMR1 (N = 75)	TCMR2 (N = 100)	*P* value for TCMR1 vs TCMR2
9 histology lesion scores					
TCMR-related	t (tubulitis)	0.30	2.19	2.00	0.09
	i (interstitial infiltrate)	0.32	2.16	1.92	0.16
All rejection-related	v (vasculitis)	0.01	**0.37**	0.07	0.0002
AMR-related	g (glomerulitis)	0.27	**0.50**	0.18	0.01
	ptc (capillaritis)	0.25	**0.32**	0.60	0.01
Atrophy-fibrosis-related	ci (scarring)	1.12	1.19	**1.77**	0.0003
	ct (atrophy)	1.03	1.09	**1.69**	0.0001
	cv (intimal thickening)	0.90	0.55	**1.04**	0.0011
	ah (arteriolar hyalinosis)	1.00	0.21	**0.73**	<0.0001
16 transcript set and molecular classifier scores					
TCMR-related classifiers	TCMR ($TCMR_{Prob}$)	0.03	**0.60**	0.24	<0.0001
	i-score ($i>1_{Prob}$) classifier	0.06	**0.84**	0.65	<0.0001
	t-score ($t>1_{Prob}$) classifier	0.06	**0.83**	0.62	<0.0001
All-rejection-related	Rej_{Prob} classifier	0.12	**0.85**	0.54	<0.0001
AMR-related	DSA-selective transcripts (DSAST)	0.07	**0.33**	0.17	<0.0001
	NK cell burden (NKB)	0.36	**1.01**	0.80	0.001
	AMR-related classifier (AMR_{Prob})	0.08	**0.30**	0.13	<0.0001
Macrophage-related	Alternatively activated macrophage (AMAT1)	0.40	**1.53**	1.23	<0.0001
	Constitutive macrophage (QCMAT)	0.31	**1.46**	1.11	<0.0001
Recent injury-related	Fibrillar collagen (FICOL)	1.11	1.61	1.58	0.72
	Injury-repair induced, day 3 (IRITD3)	0.04	0.22	0.17	0.01
	Injury-repair induced, day 5 (IRITD5)	0.33	0.64	0.59	0.09
	Injury/repair associated (IRRAT30)	0.26	1.13	0.99	0.04
	GFR_{prob}	0.32	0.60	0.52	0.05
Atrophy-fibrosis related	Fibrosis ($ci>1_{Prob}$) classifier	0.31	0.40	**0.53**	0.001
	Atrophy ($ct>1_{Prob}$) classifier	0.26	0.30	**0.46**	<0.0001

Wilcoxon *t* test was performed between TCMR1 and TCMR2 biopsies for each molecular classifier.
Gray shading indicates significant difference $P < 0.01$ between TCMR1 and TCMR2.
Bolding indicates the higher value (between TCMR1 or TCMR2) when $P < 0.05$.
AMR, antibody-mediated rejection; AMR_{Prob}, AMR-probability classifier; ci > 1Prob, ci>1-probability classifier; ct > 1Prob, ct > 1-probability classifier; DSA, donor-specific antibody; GFR, glomerular filtration rate; i > 1Prob, i > 1-probability classifier; NK, natural killer; t > 1Prob, t > 1-probability classifier; TCMR, T cell–mediated rejection; $TCMR_{Prob}$, TCMR-probability classifier.

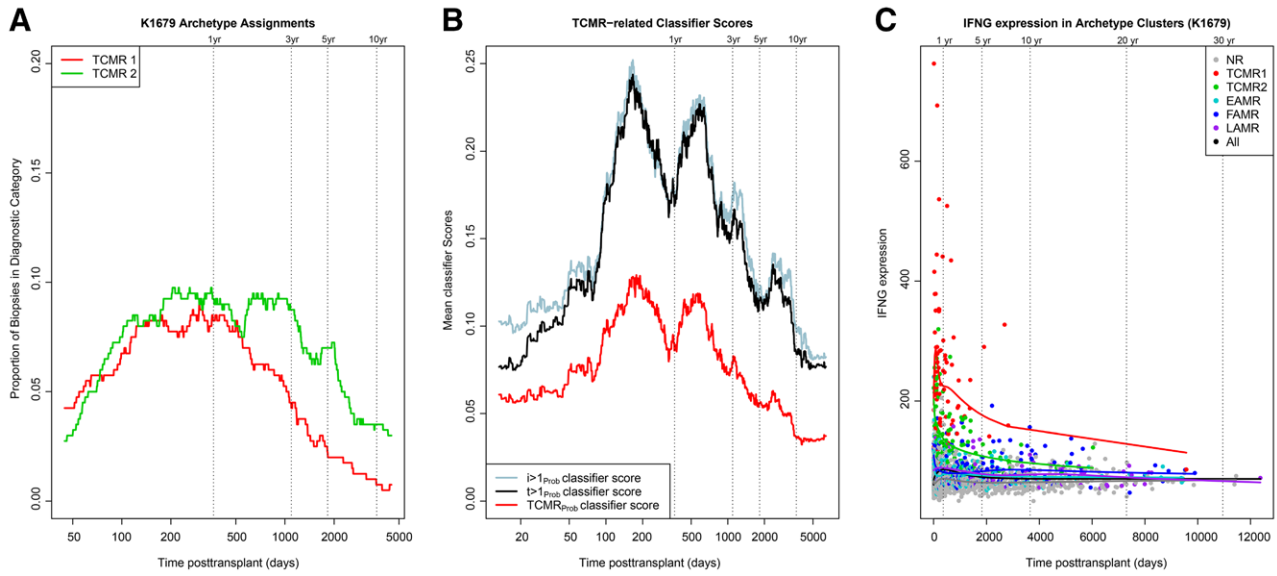

FIGURE 3. Rolling averages for the relationships between time posttransplant and the TCMR molecular classes and features in 1679 biopsies. Rolling averages over time posttransplant (A) showing the proportion of biopsies assigned TCMR1 and TCMR2 archetypes and (B) showing the TCMR-related classifier scores. (C) *IFNG* expression in archetype clusters over time posttransplant (shown as a linear scale). EAMR, early-stage molecular AMR; FAMR, fully developed molecular AMR; LAMR, late-stage molecular AMR; NR, no rejection; TCMR, T cell–mediated rejection.

TABLE 3.

Distribution of TCMR episodes (TCMR1 and TCMR2) over time intervals posttransplant

	No. of biopsies per time interval posttransplant (% of total in interval) (N out of 1679)					
	<2 m (N = 270)	2 m–1 y (N = 437)	1–5 y (N = 489)	5–10 y (N = 247)	>10 y (N = 228)	Totals per row
TCMR1	8 (3%)	35 (8%)	26 (5%)	4 (2%)	1 (0.4%)	75
TCMR2	6 (2%)	38 (7%)	40 (8%)	11 (4%)	4 (2%)	100
All TCMR (TCMR1 + TCMR2)	8 (5%)	73 (17%)	66 (13%)	15 (6%)	5 (2%)	175

TCMR, T cell–mediated rejection.

fact that TCMR1 and TCMR2 both rose, peaked, and declined showed that the TCMR1-TCMR2 gradient in disease activity and the other differences between TCMR1 and TCMR2 were not primarily because of time posttransplant. TCMR1 in particular was very rare after 10 y, occurring in only 1 of 228 biopsies (0.4%).

As a measure of TCMR activity over time within all 1679 biopsies, the TCMR-related classifiers are plotted in Figure 3B. The $TCMR_{Prob}$ classifier showed 2 peaks before a steady decline. The i-lesion and t-lesion classifiers ($i>1_{Prob}$ and $t>1_{Prob}$) trained on the histology i- and t-scores, respectively, showed similar patterns.

We studied the expression of *IFNG*, the classical cytokine induced by activation of effector T cells over time in the 1679 population. We plotted the biopsies on a linear *x*-axis to visualize the actual relationships between time and *IFNG* expression (Figure 3C). Biopsies were colored by their archetype group membership, and splines were calculated to represent the moving average of *IFNG* expression within each group. Among all biopsies, very high *IFNG* activity was an exclusive feature of the early TCMR1 biopsies. The second highest *IFNG* expression was in early TCMR2 biopsies. In both TCMR1 and TCMR2, high *IFNG* expression ceased after the first 2 y. Even FAMR (blue symbols) had much lower expression of *IFNG*, although higher than in NR biopsies. Therefore, high *IFNG* expression in early TCMR reflected TCMR intensity, not concomitant AMR.

Effect of Time Posttransplant on Disease Activity in Biopsies With TCMR

Within TCMR biopsies, we studied expression of *IFNG* and 3 other T cell–activation features—*LAG3*, *CTLA4*, and *BTLA4*—in TCMR1/2 biopsies over log time, compared with the $TCMR_{Prob}$ classifier (Figure 4A). $TCMR_{Prob}$ classifier scores (ie, TCMR activity) were high until 1 y posttransplant before progressively declining. The moving averages of *IFNG* and *LAG3* expression also showed a steady decline after 1 y; *CTLA4* and *BTLA* showed similar patterns despite lower overall expression. Despite the decline, the mean $TCMR_{Prob}$ was still elevated in late TCMR (0.3), approximately 3 times its diagnostic threshold.

The AMR_{Prob} classifier score in TCMR biopsies peaked and plateaued between 1 and 3 y. We assessed the effect of time on moving average scores for histologic lesions (i, t, v, and ci) in TCMR biopsies (Figure 4B). The i- and t-lesion scores remained relatively high around their diagnostic thresholds of 2.0 even in late TCMR, whereas v-lesions became rare. Histologic fibrosis (ci lesion scores) within TCMR steadily increased with time.

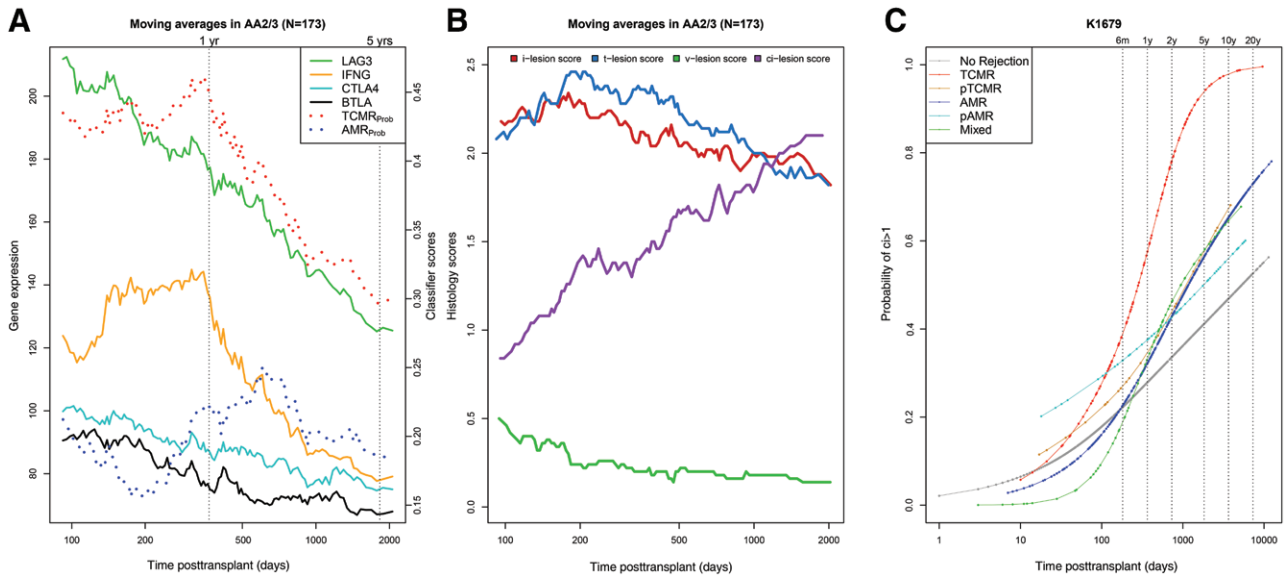

FIGURE 4. Relationships between time posttransplant and the moving average scores for molecular and histologic features of the biopsies. Two biopsies were missing date of transplant and were excluded from the time courses. (A) Molecular features and TCMR-associated gene expression within 175 TCMR biopsies. (B) Histologic lesions within 175 TCMR biopsies. (C) The probability of ci lesion scores >1 per archetype group over time posttransplant, as calculated in logistic regression. AMR, antibody-mediated rejection; pAMR, possible antibody-mediated rejection; TCMR, T cell–mediated rejection; pTCMR, possible T cell–mediated rejection.

Molecular TCMR Is Associated With Increasing Fibrosis

Fibrosis increases with time in kidney transplant biopsies, even those with NR.[33] To determine whether TCMR further increased fibrosis, we used regression analysis to compare the probability of fibrosis among different molecular rejection groups (Figure 4C). The probability of ci lesion scores >1 increased with time in all biopsies but was highest in TCMR biopsies.

The mean and median ci- and ct-scores and the $ci>1_{Prob}$ and $ct>1_{Prob}$ classifiers in biopsies before and after 1 y are detailed in Table 4. The histology ci- and ct-scores, molecular $ci>1_{Prob}$, and $ct>1_{Prob}$ classifier scores were all significantly higher in TCMR versus NR biopsies, even in the first year posttransplant. Transcript sets reflecting recent or ongoing parenchymal injury were also higher in TCMR. Therefore, biopsies with TCMR consistently display parenchymal damage, with increased scores for molecular injury and atrophy-fibrosis.

Top Transcripts Correlating With Time in Molecular TCMR Biopsies

We studied the top 20 genes that increased and decreased with time posttransplant in TCMR biopsies. Among the top genes that decreased with time in TCMR1/2 were *LAG3*, *IFNG*-inducible chemokines *CXCL9*, *CXCL10*, and *CXCL11*, and *IFNG*-inducible genes such as *GBP1*, *ANKRD22*, and *IDO1* (Table 5). *IFNG* also declined with time posttransplant (Spearman correlation coefficient –0.30, $P = 0.00008$), although it was not among the top 20 by P value. The top genes that increased in expression with time reflected atrophy-fibrosis,[34,35] including immunoglobulin transcripts representing plasma cells and mast cell transcript *CPA3* (Table 6). There was also increased expression of *SPAG4*, a gene expressed in injured renal tubule epithelial cells, inducible by hypoxia-inducible factor-1.[36] Acknowledging that the peak-plateau-decline pattern can make correlations misleading, we confirmed these findings in 86 biopsies >1 y posttransplant. The results were similar: decline in TCMR activity features (eg, *LAG3*) and rise in atrophy-fibrosis features (eg, immunoglobulin transcripts; **Tables S5 and S6, SDC**, http://links.lww.com/TP/C603).

The Correlation of Time Posttransplant With Histologic and Molecular Scores in TCMR Biopsies

Table 7 lists the correlations of histologic and molecular scores (the same scores as in Table 2) with time posttransplant in TCMR1/2 biopsies after 1 y posttransplant. Within TCMR1/2 biopsies, the defining histologic lesions

TABLE 4.

Comparing ci and ct lesion scores and classifiers in archetypal TCMR1+2 and NR before and after 1 y posttransplant

		Biopsies <1 y posttransplant			Biopsies ≥1 y posttransplant		
		TCMR175 (N=87)	No rejection (N=513)	Wilcoxon test *P* value comparing TCMR and NR	TCMR175 (N=88)	No rejection (N=526)	Wilcoxon test *P* value comparing TCMR and NR
Atrophy-fibrosis lesion scores	Mean (median) ci lesion score	1.08 (1.0)	0.81 (1.0)	0.025	1.86 (2.0)	1.39 (1.0)	0.0001
	Mean (median) ct lesion score	1.03 (1.0)	0.72 (1.0)	0.0078	1.83 (2.0)	1.34 (1.0)	4.2E–5
Atrophy-fibrosis classifiers	Mean (median) ci classifier	0.40 (0.36)	0.22 (0.15)	6.6E–11	0.54 (0.53)	0.41 (0.34)	6.3E–6
	Mean (median) ct classifier	0.32 (0.24)	0.17 (0.10)	9.5E–9	0.46 (0.43)	0.35 (0.27)	5.4E–5

NR, no rejection; TCMR, T cell–mediated rejection.

TABLE 5.

Top 20 genes by Spearman correlation decreased (negatively correlated) with time posttransplant within molecular TCMR biopsies (archetypes TCMR1/2; N = 175)

Gene symbol	Gene name	Transcript set	Spearman correlation with time posttransplant[a]
CXCL9	Chemokine (C-X-C motif) ligand 9	IFNG-inducible	–0.50
GBP1	Guanylate binding protein 1, interferon-inducible	IFNG-inducible	–0.45
CXCL10	Chemokine (C-X-C motif) ligand 10	IFNG-inducible	–0.44
LAG3	Lymphocyte-activation gene 3	T cell–activation gene; TCMR-RAT	–0.44
ANKRD22	Ankyrin repeat domain 22	IFNG-inducible	–0.44
APOL4	Apolipoprotein L, 4	IFNG-inducible	–0.43
CXCL11	Chemokine (C-X-C motif) ligand 11	IFNG-inducible	–0.42
NUSAP1	Nucleolar and spindle associated protein 1	Macrophage; injury-induced (IRITD5)	–0.42
IDO1	Indoleamine 2,3-dioxygenase 1	IFNG-inducible	–0.41
GBP4	Guanylate binding protein 4	IFNG-inducible	–0.41
BATF2	Basic leucine zipper transcription factor, ATF-like 2	IFNG-inducible	–0.41
RGL1	Ral guanine nucleotide dissociation stimulator-like 1	Macrophage gene	–0.40
SMCO4	Single-pass membrane protein with coiled-coil domains 4	IFNG-inducible (macrophages)	–0.40
TAP1	Transporter 1, ATP-binding cassette, subfamily B (MDR)	IFNG-inducible	–0.40
FBXO6	F-box protein 6	IFNG-inducible	–0.40
FAM72A	Family with sequence similarity 72, member A	T cell–activation gene; TCMR-RAT	–0.39
MOB1A	MOB kinase activator 1A	Injury-induced (cIRIT)	–0.39
GABBR1	Gamma-aminobutyric acid B receptor, 1	All rejection	–0.39
IL31RA	Interleukin 31 receptor A	IFNG-inducible	–0.39
RRM2	Ribonucleotide reductase M2	Injury-induced, IRIT5	–0.39

Pseudogenes have been deleted.
PBTs are listed on our home page https://www.ualberta.ca/medicine/institutes-centres-groups/atagc/research/gene-lists.
[a]All *P* values <0.001.
PBT, pathogenesis-based transcript; TCMR, T cell–mediated rejection.

TABLE 6.

Top 20 genes by Spearman correlation increased (positively correlated) with time posttransplant within molecular TCMR biopsies (archetypes TCMR1/2; N = 175)

Gene symbol	Gene name	PBT	Spearman correlation with time posttransplant[a]
IGHG1	Immunoglobulin heavy constant gamma 1 (G1m marker)	IGT	0.51
IGHG1	Immunoglobulin heavy constant gamma 1 (G1m marker)	IGT	0.50
IGHG1	Immunoglobulin heavy constant gamma 1 (G1m marker)	IGT	0.50
IGHG1	Immunoglobulin heavy constant gamma 1 (G1m marker)	IGT	0.50
IGHG1	Immunoglobulin heavy constant gamma 1 (G1m marker)	IGT	0.50
IGHG1	Immunoglobulin heavy constant gamma 1 (G1m marker)	IGT	0.50
IGHG3	Immunoglobulin heavy constant gamma 3 (G3m marker)	IGT	0.49
IGKC	Immunoglobulin κ constant	IGT	0.48
IGKV1–39	Immunoglobulin κ variable 1–39 (gene)	IGT	0.48
RGS13	Regulator of G-protein signaling 13	B cells, mast cells	0.48
CPA3	Carboxypeptidase A3 (mast cell)	MCAT mast cells	0.47
TPSAB1	Tryptase alpha		0.47
IGH	Immunoglobulin heavy locus	IGT	0.47
SPAG4[b]	Sperm-associated antigen 4	RPTECs; induced by HIF1	0.46
IGKV1–5	Immunoglobulin κ variable 1–5	IGT	0.46
TPSAB1	Tryptase alpha		0.46
IGHG1	Immunoglobulin heavy constant gamma 1 (G1m marker)	IGT	0.46
IGK	Immunoglobulin κ locus	IGT	0.46
MS4A2	Membrane-spanning 4-domains, subfamily A, member 2	Mast cells	0.45
FCRL5	Fc receptor-like 5	BAT (B cells)	0.45

PBTs are listed on our home page https://www.ualberta.ca/medicine/institutes-centres-groups/atagc/research/gene-lists.
[a]All *P* values <0.001.
[b]SPAG4 is expressed in renal epithelial cell line and highly increased in injured kidneys.
HIF1, hypoxia-inducible factor-1; IGT, immunoglobulin transcript; PBT, pathogenesis-based transcript; RPTEC, renal proximal tubular epithelial cell; TCMR, T cell–mediated rejection.

TABLE 7.

Correlation between histology lesion scores, molecular transcript set scores, and molecular classifier scores with time of biopsy posttransplant in molecular TCMR biopsies >1 y (N = 86)[a]

		Spearman correlation with time posttransplant	*P*
9 histology lesion scores			
TCMR related	t (tubulitis)	–0.17	0.17
	i (interstitial infiltrate)	–0.14	0.27
AMR related	g (glomerulitis)	–0.13	0.29
	ptc (capillaritis)	–0.15	0.25
All rejection related	v (vasculitis)	–0.21	0.10
Atrophy-fibrosis related	ci (scarring)	**0.30**	**0.02**
	ct (atrophy)	**0.34**	**0.01**
	cv (intimal thickening)	**0.32**	**0.01**
	ah (hyalinosis)	**0.65**	**<0.001**
16 transcript set scores and classifier scores			
TCMR related classifiers	TCMR ($TCMR_{Prob}$)	**–0.27**	**0.01**
	i-score ($i > 1_{Prob}$) classifier	**–0.32**	**0.003**
	t-score ($t > 1_{Prob}$) classifier	**–0.37**	**0.0006**
All rejection related	$Rejection_{Prob}$ classifier	–0.29	0.01
AMR related	DSA-selective transcripts (DSAST)	–0.07	0.53
	NK cell burden (NKB)	0.06	0.61
	AMR (AMR_{Prob}) classifier	–0.17	0.11
Macrophage related[b]	Alternatively activated macrophage (AMAT1)	–0.08	0.45
	Constitutive macrophage (QCMAT)	–0.15	0.17
Recent injury related[c]	Fibrillar collagen (FICOL)	0.07	0.55
	Injury-repair induced, day 3 (IRITD3)	0.09	0.41
	Injury-repair induced, day 5 (IRITD5)	0.12	0.28
	Injury/repair associated (human kidney) (IRRAT30)	0.14	0.19
	Low GFR_{prob}	0.13	0.23
Atrophy-fibrosis related	Fibrosis ($ci > 1_{Prob}$)	**0.34**	**0.002**
	Atrophy ($ct > 1_{Prob}$)	**0.33**	**0.002**

PBTs are listed on our home page https://www.ualberta.ca/medicine/institutes-centres-groups/atagc/research/gene-lists.
[a]Shading and bold indicate significant association of the score with time $P < 0.05$.
[b]All macrophage-related classifier scores were significantly different between TCMR biopsies (N = 175) and NR biopsies (N = 1040) ($P < 10^{-16}$).
[c]All injury-associated classifier scores were significantly different between TCMR biopsies (N = 175) and NR biopsies (N = 1040) ($P < 10^{-11}$).
AMR, antibody-mediated rejection; $ci > 1_{Prob}$, ci > 1-probability classifier; $ct > 1_{Prob}$, ct > 1-probability classifier; DSA, donor-specific antibody; GFR, glomerular filtration rate; NK, natural killer; PBT, pathogenesis-based transcript; TCMR, T cell–mediated rejection.

of TCMR—the t- and i-scores—showed no significant change over time, that is, remained near diagnostic levels even in late TCMR biopsies, whereas v-lesions in late TCMR became uncommon. Atrophy-fibrosis–related changes were increased in later TCMR biopsies.

Among molecular scores, TCMR activity scores declined, and atrophy-fibrosis scores increased. However, recent molecular injury and macrophage transcript sets (which are abnormal in all TCMR) showed little change with time. Like tubulitis, parenchymal injury scores were consistently elevated even in late TCMR biopsies. AMR-related scores and AMR_{Prob} in TCMR biopsies did not decrease significantly. In summary, with increasing time posttransplant, molecular TCMR showed decreased molecular TCMR activity and increased atrophy/fibrosis but consistently displayed molecular injury and tubulitis.

Checkpoint Transcripts

We considered whether the gradient in disease activity between TCMR1-TCMR2 and the decline in TCMR activity over time might be associated with increased expression of immunologic checkpoint transcripts in the biopsies. Table 8 shows the correlations of selected checkpoint transcripts with time posttransplant in TCMR biopsies and compares their expression in TCMR1, TCMR2, and NR. No checkpoint transcripts increased with time: all were associated with TCMR activity and thus decreased in expression at least slightly with time, 3 significantly (*LAG*, *CTLA4*, and *BTLA*). All checkpoints were higher in TCMR1 than TCMR2. Declining TCMR activity over time and differences in TCMR activity between TCMR1 and TCMR2 were not associated with higher expression of checkpoint transcripts in the biopsy.

Kidney Graft Survival After TCMR Diagnoses in the Biopsy

We investigated 3 y postbiopsy graft loss in the 1679 cohort, selecting 1 random biopsy per group (Figure 5). In Figure 5A, TCMR1 and TCMR2 both showed increased probability of graft loss compared with NR. (EAMR showed relatively little graft loss in the first 2 y, as previously reported.[21,22] We assessed the relative importance

TABLE 8.

Expression of checkpoint transcripts in TCMR archetypes (N = 175) in relationship with time posttransplant and to class comparison between TCMR1 and TCMR2

	Correlation with time posttransplant			Comparing expression in TCMR1 vs TCMR2					
Checkpoints and ligands	Rank by *P*	Spearman correlation coefficient	*P*	Rank by *P*	TCMR1	TCMR2	No rejection	*P*	Adjusted *P*
TIGIT[a]	11 643	–0.13	NS	66	165	94	43	**9.41E–16**	7.05E–13
BTLA	3193	–0.20	**0.008**	5446	91	70	19	**0.004**	0.04
CTLA4	2351	–0.22	**0.004**	275	58	39	22	**3.11E–11**	5.59E–09
PDCD1	12 630	–0.12	NS	433	101	82	75	**1.05E–09**	1.20E–07
CD160[b]	11 579	–0.13	NS	3607	72	53	25	**0.001**	0.01
LAG3	32	–0.44	**1.0E–09**	33	232	132	66	**7.48E–18**	1.12E–14
CD244/2B4	32 205	–0.05	NS	768	54	43	29	**6.80E–08**	4.38E–06
HAVCR2/TIM3	35 399	–0.04	NS	336	42	29	20	**1.37E–10**	2.02E–08
TNFSF9/CD137	7967	–0.15	NS	7	72	35	17	**8.75E–21**	6.03E–17

[a]Bold and shaded are checkpoints that do not decrease in expression significantly with time but are higher in TCMR1 than TCMR2.
[b]CD160 is included because it is a marker for exhausted T cells.
NS, not significant; TCMR, T cell–mediated rejection.

of various molecular scores in the biopsy for predicting short-term (3 y) graft survival after the diagnosis of TCMR (Figure 5B). The strongest molecular feature predicting graft survival was recent or ongoing parenchymal injury, that is, the lowGFR$_{Prob}$ classifier score and the Injury repair response-associated transcripts transcript set, both measures of recent injury. Thus, in biopsies with molecular TCMR, the TCMR activity-related features were relatively unimportant once parenchymal injury features were included in the multivariable random forest analysis.

Associations With Intimal Arteritis

Because molecular diagnoses are not influenced by the presence of histologic v-lesions, we could study the relationship between associations between v-lesions and molecular diagnoses (Table 9). In 1337 biopsies in which v-lesions could be scored, v-lesions >0 were recorded in 51 (4%), mostly v1. By archetypes, most v-lesions were in biopsies with TCMR1, FAMR, or NR biopsies. This is compatible with the previous conclusion that v-lesions can reflect AMR, TCMR, or injury.[20,37]

Impact of BKN

BKN often has TCMR-like changes, directed at alloantigens, viral antigens, or both.[9,38-43] In the 175 TCMR biopsies, 3 TCMR1 and 21 TCMR2 biopsies were diagnosed locally as BKN. The conclusions from the abovementioned analyses did not change when BKN biopsies were excluded. Details of the BKN biopsies have been published previously.[9]

DISCUSSION

We studied the variation in molecular and histologic features in molecular TCMR to understand the determinants of intensity and the effect of time posttransplant. Defining TCMR molecularly using automatically assigned archetypes permitted us to study the relationships between molecular TCMR activity (as defined by the TCMR

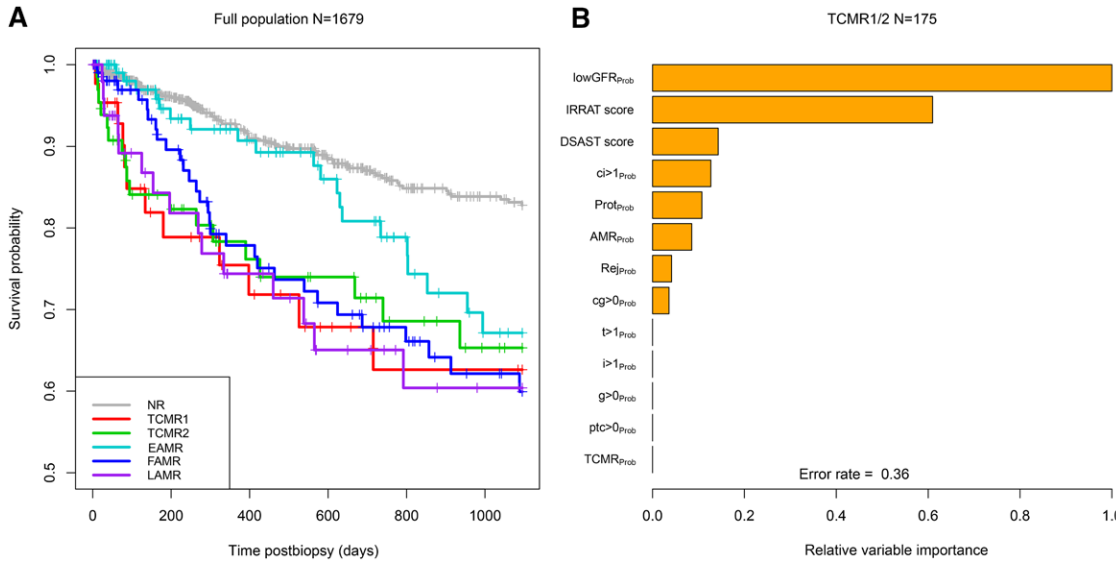

FIGURE 5. Survival analysis during 3 y postbiopsy (days), with 1 random biopsy per patient. (A) Actuarial survival curves by archetype group. (B) Random forests showing the variable importance (including molecular and histologic features) in the prediction of 3 y postbiopsy graft survival. TCMR, T cell–mediated rejection.

TABLE 9.

Number of biopsies with v-lesions in N = 1679 biopsies that could be scored for v-lesions (histology not shown because it uses v-lesions for classification)

		v-lesion score				
		0	1	2	3	All v > 0
Rejection archetype groups	No rejection	816	8	1	0	9
	TCMR1	44	12	2	2	16
	TCMR2	70	3	1	0	4
	EAMR	169	5	1	0	6
	FAMR	130	9	4	1	14
	LAMR	57	1	1	0	2
	Total	1286	38	10	3	51

EAMR, early-stage molecular AMR; FAMR, fully developed molecular AMR; LAMR, late-stage molecular AMR; TCMR, T cell–mediated rejection.

classifier scores) and histologic lesions without using the lesions to make the TCMR diagnosis. In 175 molecular TCMR biopsies, there was a strong gradient of disease activity between TCMR1 and TCMR2: TCMR1 had higher TCMR activity, more AMR activity (mixed rejection), and more frequent v-lesions but little hyalinosis, whereas TCMR2 had more atrophy-fibrosis. However, TCMR1 and TCMR2 had similar molecular injury and tubulitis. Time had strong effects on the frequency of TCMR as previously described[12] and also affected disease activity in the TCMR biopsies that did occur. TCMR biopsies after 1 y posttransplant showed progressively less molecular TCMR classifier activity and decreased expression of effector T-cell activity molecules such as *IFNG* and *LAG3*. TCMR was associated with increased probability of atrophy-fibrosis even within the first year. However, like the TCMR1-TCMR2 gradient, molecular injury and tubulitis were consistently present in TCMR, with tubulitis remaining at diagnostic levels (t2) even in late TCMR with atrophy-fibrosis. TCMR increased the probability of graft loss, and in random forests, the risk of loss after biopsies with TCMR correlated most strongly with recent or ongoing parenchymal injury, not TCMR activity. We conclude that TCMR biopsies display a reciprocal relationship between TCMR molecular activity and the extent of hyalinosis and fibrosis and that time posttransplant beyond 1 y is associated with attenuated molecular activity and increased fibrosis in TCMR. Nevertheless, molecular injury and tubulitis were always present in TCMR, and injury and atrophy-fibrosis, not TCMR activity, determined the risk of graft failure with 3 y postbiopsy.

The striking reciprocal relationship between TCMR activity, hyalinosis, and fibrosis suggests that underexposure to CNIs for a considerable time before the biopsy likely contributes to the TCMR1-TCMR2 gradient. This can only be proven by detailed studies of drug exposure in the months before biopsy and is not feasible in routine clinical practice. Single-drug levels at the time of indication biopsy are not informative because low levels, once detected at a clinic visit, will often be corrected before the biopsy.

It is a testament to the robustness of the original Banff definition of TCMR that, despite their heterogeneity, all molecular TCMRs, even late TCMR, manifest i- and t-lesions. Tubulitis, with its accompanying interstitial mononuclear infiltrate, emerges as a reflection of the parenchymal injury induced by TCMR and a universal feature of molecular TCMR regardless of time posttransplant. Increasing atrophy-fibrosis can interfere with assignment of t-scores. Nevertheless, mean tubulitis scores were at diagnostic levels even late posttransplant, accompanied by molecular features of recent or ongoing injury: injury-induced transcript sets, macrophage transcripts, and the $lowGFR_{Prob}$ injury classifier.

These results cannot resolve the debate over whether tubulitis in atrophic tubules should be interpreted as a "chronic-active TCMR" phenotype, separate from the usual TCMR definition based on tubulitis. The concept of chronic-active TCMR based on inflammation in atrophy-fibrosis lesions in biopsies lacking tubulitis was introduced in Banff 2015[44] but has been controversial.[44-48] Definitions of chronic-active TCMR were revised in Banff 2017[48] to require moderate or severe tubulitis and will be revisited in Banff 2022.[46,47,49] Inflammation in atrophy-fibrosis lesions is a general feature of progressive nephron injury, even in primary renal diseases in native kidneys, and strongly related to future transplant failure.[50,51] Our finding that mean tubulitis scores remain at or near diagnostic levels in late molecular TCMR is reassuring, but it would be useful to identify and validate histologic features indicating TCMR when the atrophy-fibrosis is too extensive for reliable tubulitis assessment. Calibrating candidate criteria against molecular TCMR activity scores could be useful in this process.

The cognate T cells that generate effector T cells in the secondary lymphoid organs are programmed to undergo exhaustion when they face persistent antigen,[12,52-60] and we believe that this probably contributes to the time-related decline in TCMR activity, as well as TCMR frequency. Immunologic checkpoints are involved in this adaptation because checkpoint inhibition to treat cancer in transplant patients frequently triggers intense TCMR.[61-63] The observation that checkpoint gene expression in the biopsy does not correlate with low TCMR activity or increase with time does not imply that checkpoints are not operating, given the complexity of the mechanisms that are implicated in the exhaustion phenotype.[64,65] Moreover, analysis of an indication biopsy cohort has a limited ability to draw conclusions about the role of checkpoints because the patients with the strongest influence of checkpoints (ie, who have NR) will presumably not get rejection and thus will not be represented in an indication biopsy population. We also emphasize that we have not been able to find specific features of T cell exhaustion in the biopsies in this study.

TCMR is usually thought of as "episodes," but its association with fibrosis suggests that TCMR is often a smoldering process for long periods before it is recognized, injuring nephrons (tubulitis) and driving atrophy-fibrosis. Multiple TCMR episodes increase the risk of graft loss,[5] raising the possibility of unrecognized TCMR operating in patients between episodes. We need to determine whether our current treatments fully reverse cognate T cell–mediated inflammation and whether such treatments then arrest nephron loss and atrophy-fibrosis. It is also possible that, even if effector T cell activity is sterilized, the damaged nephron epithelium is programmed to progress to failure, reminiscent of the changes that occur in skin epithelia where injury programs epigenetic changes in stem cells to "remember" inflammation.[66]

The deleterious impact of TCMR on graft survival in the 1679 population differed somewhat from earlier findings in the first 703 biopsies,[12] which showed a strong impact of AMR and mixed rejection but less impact of "pure" TCMR on survival. Greater numbers and longer follow-up in the present cohort make the damaging effect of pure TCMR clear.

There is strong agreement between MMDx and histology, despite histology using different fragments of tissue. Each uses a sample that is sufficient to give an estimate of the rejection state in the kidney, and there is no need for MMDx to read the same tissue pieces as histology. MMDx requires less tissue (0.3–0.5 mm of a core) because molecular changes (eg, IFNG effects) are more diffuse than histologic changes, and we have outlined reasons for confidence in MMDx when the 2 differ.[4] Variation between pieces in MMDx measurements is much less than the variation between pathologists, because of the interobserver variation ("noise") in histology assessments,[1] and disagreement between MMDx and histology is about what is expected from this noise. It is reassuring that MMDx provides significantly better agreement with external measurements such as donor-derived cell-free DNA.[67-69]

The strong association of TCMR with parenchymal injury and atrophy-fibrosis and the crucial role of injury rather than TCMR activity in determining outcome after TCMR biopsies underscores the need to emphasize prevention of TCMR rather than simply trying to suppress TCMR activity by treatment. The increased atrophy-fibrosis within TCMR is presumably a consequence of the nephron injury that is manifested as increased molecular injury-induced transcripts and histologically as tubulitis. TCMR directly damages the nephron epithelium, accompanied by major structural changes such as loss of cadherins.[70] This contrasts with AMR, a microcirculation disease that usually spares the parenchyma until glomerular damage accumulates and triggers shutdown, giving EAMR its relatively benign short-term prognosis.[21,22] We believe that nephrons that have experienced TCMR injury and tubulitis may be programmed for irreversible shutdown (atrophy), again stressing the need for prevention. Based on the finding of under-hyalinosis in TCMR1 and even in TCMR2 to some extent, this suggests a renewed emphasis on maintaining adequate immunosuppression. However, we recognize the fact that hyalinosis has poor κ values in histology[71] and that many confounders (eg, associations with aging, glomerulonephritis, glomerular sclerosis, and atrophy-fibrosis) limit the usefulness of under-hyalinosis in histologic diagnosis of individual biopsies.

ACKNOWLEDGMENTS

The authors thank our valued clinicians in the INTERCOMEX study group who partnered with us for this study by contributing biopsies and feedback (Harold Yang, Seth Narins, Carmen Lefaucheur, Alexandre Loupy, Bertram Kasiske, Arthur Matas, and Arjang Djamali).

REFERENCES

1. Halloran PF. Immunosuppressive drugs for kidney transplantation. *N Engl J Med*. 2004;351:2715–2729.
2. Ekberg H, Tedesco-Silva H, Demirbas A, et al; ELITE-Symphony Study. Reduced exposure to calcineurin inhibitors in renal transplantation. *N Engl J Med*. 2007;357:2562–2575.
3. Einecke G, Sis B, Reeve J, et al. Antibody-mediated microcirculation injury is the major cause of late kidney transplant failure. *Am J Transplant*. 2009;9:2520–2531.
4. Madill-Thomsen K, Perkowska-Ptasińska A, Böhmig GA, et al; MMDx-Kidney Study Group. Discrepancy analysis comparing molecular and histology diagnoses in kidney transplant biopsies. *Am J Transplant*. 2020;20:1341–1350.
5. Rampersad C, Balshaw R, Gibson IW, et al. The negative impact of T cell-mediated rejection on renal allograft survival in the modern era. *Am J Transplant*. 2022;22:761–771.
6. Cosio FG, Lager DJ, Lorenz EC, et al. Significance and implications of capillaritis during acute rejection of kidney allografts. *Transplantation*. 2010;89:1088–1094.
7. Sellarés J, de Freitas DG, Mengel M, et al. Understanding the causes of kidney transplant failure: the dominant role of antibody-mediated rejection and nonadherence. *Am J Transplant*. 2012;12:388–399.
8. Hricik DE, Formica RN, Nickerson P, et al; Clinical Trials in Organ Transplantation-09 Consortium. Adverse outcomes of tacrolimus withdrawal in immune-quiescent kidney transplant recipients. *J Am Soc Nephrol*. 2015;26:3114–3122.
9. Halloran PF, Madill-Thomsen KS, Böhmig GA, et al; INTERCOMEX Investigators. A 2-fold approach to polyoma virus (BK) nephropathy in kidney transplants: distinguishing direct virus effects from cognate T cell-mediated inflammation. *Transplantation*. 2021;105:2374–2384.
10. Einecke G, Reeve J, Halloran PF. Hyalinosis lesions in renal transplant biopsies: time-dependent complexity of interpretation. *Am J Transplant*. 2017;17:1346–1357.
11. Einecke G, Reeve J, Halloran PF. A molecular biopsy test based on arteriolar under-hyalinosis reflects increased probability of rejection related to under-immunosuppression. *Am J Transplant*. 2018;18:821–831.
12. Halloran PF, Chang J, Famulski K, et al. Disappearance of T cell-mediated rejection despite continued antibody-mediated rejection in late kidney transplant recipients. *J Am Soc Nephrol*. 2015;26:1711–1720.
13. Burke JF Jr, Pirsch JD, Ramos EL, et al. Long-term efficacy and safety of cyclosporine in renal-transplant recipients. *N Engl J Med*. 1994;331:358–363.
14. Meier-Kriesche HU, Steffen BJ, Hochberg AM, et al. Long-term use of mycophenolate mofetil is associated with a reduction in the incidence and risk of late rejection. *Am J Transplant*. 2003;3:68–73.
15. Ooi BS, Jao W, First MR, et al. Acute interstitial nephritis. A clinical and pathologic study based on renal biopsies. *Am J Med*. 1975;59:614–628.
16. Sibley RK, Rynasiewicz J, Ferguson RM, et al. Morphology of cyclosporine nephrotoxicity and acute rejection in patients immunosuppressed with cyclosporine and prednisone. *Surgery*. 1983;94:225–234.
17. Verani RR, Flechner SM, Van Buren CT, et al. Acute cellular rejection or cyclosporine a nephrotoxicity? A review of transplant renal biopsies. *Am J Kidney Dis*. 1984;4:185–191.
18. Beschorner WE, Burdick JF, Williams GM, et al. The presence of leu-7 reactive lymphocytes in renal-allografts undergoing acute rejection. *Transplant Proc*. 1985;17:618–622.
19. Solez K, Axelsen RA, Benediktsson H, et al. International standardization of criteria for the histologic diagnosis of renal allograft rejection: the Banff working classification of kidney transplant pathology. *Kidney Int*. 1993;44:411–422.
20. Salazar ID, Merino López M, Chang J, et al. Reassessing the significance of intimal arteritis in kidney transplant biopsy specimens. *J Am Soc Nephrol*. 2015;26:3190–3198.
21. Reeve J, Böhmig GA, Eskandary F, et al; MMDx-Kidney study group. Assessing rejection-related disease in kidney transplant biopsies based on archetypal analysis of molecular phenotypes. *JCI Insight*. 2017;2:94197.
22. Halloran PF, Madill-Thomsen KS, Pon S, et al; INTERCOMEX Investigators. Molecular diagnosis of ABMR with or without donor-specific antibody in kidney transplant biopsies: differences in timing and intensity but similar mechanisms and outcomes. *Am J Transplant*. 2022;22:1976–1991.
23. Reeve J, Sellarés J, Mengel M, et al. Molecular diagnosis of T cell-mediated rejection in human kidney transplant biopsies. *Am J Transplant*. 2013;13:645–655.
24. Venner JM, Famulski KS, Badr D, et al. Molecular landscape of T cell-mediated rejection in human kidney transplants: prominence of CTLA4 and PD ligands. *Am J Transplant*. 2014;14:2565–2576.
25. Madill-Thomsen KS, Böhmig GA, Bromberg J, et al; INTERCOMEX Investigators. Donor-specific antibody is associated with increased

expression of rejection transcripts in renal transplant biopsies classified as no rejection. *J Am Soc Nephrol*. 2021;32:2743–2758.
26. Halloran PF, Reeve J, Akalin E, et al. Real time central assessment of kidney transplant indication biopsies by microarrays: the INTERCOMEX study. *Am J Transplant*. 2017;17:2851–2862.
27. Reeve J, Böhmig GA, Eskandary F, et al; INTERCOMEX MMDx-Kidney Study Group. Generating automated kidney transplant biopsy reports combining molecular measurements with ensembles of machine learning classifiers. *Am J Transplant*. 2019;19:2719–2731.
28. Reeve J, Madill-Thomsen KS, Halloran PF, et al. Using ensembles of machine learning classifiers to maximize the accuracy and stability of molecular biopsy interpretation. *Am J Transplant*. 2019;19(S3): 452–453.
29. Lê S, Josse J, Husson F. FactoMineR: AnRPackage for multivariate analysis. *J Stat Software*. 2008;25:18.
30. Smythe GK. limma: linear models for microarray data. In: Gentleman RHW, Carey VJ, Irizarry RA, and Dudoit S, eds. *Bioinformatics and Computational Biology Solutions using R and Bioconductor*. Springer; 2005:398–420.
31. Therneau T. *A package for survival analysis in R*. Published 2020. Available at https://CRAN.R-project.org/package=survival. Accessed March 1, 2022.
32. Harrell, F. E., Jr. *rms: regression modeling strategies. R package version 6.0-0*. 2020. Available at https://CRAN.R-project.org/package=rms [computer program]. Accessed March 6, 2022.
33. Venner JM, Famulski KS, Reeve J, et al. Relationships among injury, fibrosis, and time in human kidney transplants. *JCI Insight*. 2016;1:e85323.
34. Einecke G, Reeve J, Mengel M, et al. Expression of B cell and immunoglobulin transcripts is a feature of inflammation in late allografts. *Am J Transplant*. 2008;8:1434–1443.
35. Mengel M, Reeve J, Bunnag S, et al. Molecular correlates of scarring in kidney transplants: the emergence of mast cell transcripts. *Am J Transplant*. 2009;9:169–178.
36. Shoji K, Murayama T, Mimura I, et al. Sperm-associated antigen 4, a novel hypoxia-inducible factor 1 target, regulates cytokinesis, and its expression correlates with the prognosis of renal cell carcinoma. *Am J Pathol*. 2013;182:2191–2203.
37. Reeve J, Einecke G, Mengel M, et al. Diagnosing rejection in renal transplants: a comparison of molecular- and histopathology-based approaches. *Am J Transplant*. 2009;9:1802–1810.
38. Hirsch HH, Brennan DC, Drachenberg CB, et al. Polyomavirus-associated nephropathy in renal transplantation: interdisciplinary analyses and recommendations. *Transplantation*. 2005;79:1277–1286.
39. Johnston O, Jaswal D, Gill JS, et al. Treatment of polyomavirus infection in kidney transplant recipients: a systematic review. *Transplantation*. 2010;89:1057–1070.
40. Masutani K, Shapiro R, Basu A, et al. Putative episodes of T-cell-mediated rejection in patients with sustained BK viruria but no viremia. *Transplantation*. 2012;94:43–49.
41. Schmid H, Nitschko H, Gerth J, et al. Polyomavirus DNA and RNA detection in renal allograft biopsies: results from a European multicenter study. *Transplantation*. 2005;80:600–604.
42. Stervbo U, Nienen M, Hecht J, et al. Differential diagnosis of interstitial allograft rejection and BKV nephropathy by T-cell receptor sequencing. *Transplantation*. 2020;104:e107–e108.
43. Trydzenskaya H, Sattler A, Müller K, et al. Novel approach for improved assessment of phenotypic and functional characteristics of BKV-specific T-cell immunity. *Transplantation*. 2011;92:1269–1277.
44. Loupy A, Haas M, Solez K, et al. The banff 2015 kidney meeting report: current challenges in rejection classification and prospects for adopting molecular pathology. *Am J Transplant*. 2017;17:28–41.
45. Halloran PF, Chang J, Famulski KS. Inflammation in scarred areas (i-IFTA) is a reflection of parenchymal injury (response to wounding) not T cell-mediated rejection. *Am J Transplant*. 2018;18(S4): 328–328.
46. Halloran PF, Matas A, Kasiske BL, et al. Molecular phenotype of kidney transplant indication biopsies with inflammation in scarred areas. *Am J Transplant*. 2019;19:1356–1370.
47. Helgeson ES, Mannon R, Grande J, et al. i-IFTA and chronic active T cell-mediated rejection: a tale of 2 (DeKAF) cohorts. *Am J Transplant*. 2021;21:1866–1877.
48. Haas M, Loupy A, Lefaucheur C, et al. The Banff 2017 kidney meeting report: revised diagnostic criteria for chronic active T cell-mediated rejection, antibody-mediated rejection, and prospects for integrative endpoints for next-generation clinical trials. *Am J Transplant*. 2018;18:293–307.
49. Naesens M, Haas M, Loupy A, et al. Does the definition of chronic active T cell-mediated rejection need revisiting? *Am J Transplant*. 2021;21:1689–1690.
50. Nankivell BJ, Shingde M, Keung KL, et al. The causes, significance and consequences of inflammatory fibrosis in kidney transplantation: the Banff i-IFTA lesion. *Am J Transplant*. 2017;18:364–376.
51. Lefaucheur C, Gosset C, Rabant M, et al. T cell-mediated rejection is a major determinant of inflammation in scarred areas in kidney allografts. *Am J Transplant*. 2018;18:377–390.
52. Manohar S, Thongprayoon C, Cheungpasitporn W, et al. Systematic review of the safety of immune checkpoint inhibitors among kidney transplant patients. *Kidney Int Rep*. 2020;5:149–158.
53. Abdel-Wahab N, Safa H, Abudayyeh A, et al. Checkpoint inhibitor therapy for cancer in solid organ transplantation recipients: an institutional experience and a systematic review of the literature. *J Immunother Cancer*. 2019;7:106.
54. Mroue A, Moujaess E, Kourie HR, et al. Exploring the knowledge gap of immune checkpoint inhibitors in chronic renal failure: a systematic review of the literature. *Crit Rev Oncol Hematol*. 2021;157:103169.
55. Adam BA, Murakami N, Reid G, et al. Gene expression profiling in kidney transplants with immune checkpoint inhibitor-associated adverse events. *Clin J Am Soc Nephrol*. 2021;16:1376–1386.
56. Mejia CD, Frank AM, Singh P, et al. Immune checkpoint inhibitor therapy-associated graft intolerance syndrome in a failed kidney transplant recipient. *Am J Transplant*. 2021;21:1322–1325.
57. Nguyen LS, Ortuno S, Lebrun-Vignes B, et al. Transplant rejections associated with immune checkpoint inhibitors: a pharmacovigilance study and systematic literature review. *Eur J Cancer*. 2021;148:36–47.
58. Venkatachalam K, Malone AF, Heady B, et al. Poor outcomes with the use of checkpoint inhibitors in kidney transplant recipients. *Transplantation*. 2020;104:1041–1047.
59. Jose A, Yiannoullou P, Bhutani S, et al. Renal allograft failure after ipilimumab therapy for metastatic melanoma: a case report and review of the literature. *Transplant Proc*. 2016;48:3137–3141.
60. Lesouhaitier M, Dudreuilh C, Tamain M, et al. Checkpoint blockade after kidney transplantation. *Eur J Cancer*. 2018;96:111–114.
61. Zwald FO. Transplant-associated cancer in the era of immune checkpoint inhibitors: primum non nocere. *Am J Transplant*. 2020;20:2299–2300.
62. d'Izarny-Gargas T, Durrbach A, Zaidan M. Efficacy and tolerance of immune checkpoint inhibitors in transplant patients with cancer: a systematic review. *Am J Transplant*. 2020;20:2457–2465.
63. Lipson EJ, Bagnasco SM, Moore J Jr, et al. Tumor regression and allograft rejection after administration of anti-PD-1. *N Engl J Med*. 2016;374:896–898.
64. Im SJ, Ha SJ. Re-defining T-cell exhaustion: subset, function, and regulation. *Immune Netw*. 2020;20:e2.
65. Blank CU, Haining WN, Held W, et al. Defining 'T cell exhaustion'. *Nat Rev Immunol*. 2019;19:665–674.
66. Naik S, Larsen SB, Gomez NC, et al. Inflammatory memory sensitizes skin epithelial stem cells to tissue damage. *Nature*. 2017;550: 475–480.
67. Halloran PF, Reeve J, Madill-Thomsen KS, et al; Trifecta Investigators. The trifecta study: comparing plasma levels of donor-derived cell-free DNA with the molecular phenotype of kidney transplant biopsies. *J Am Soc Nephrol*. 2022;33:387–400.
68. Gupta G, Moinuddin I, Kamal L, et al. Correlation of donor-derived cell-free DNA with histology and molecular diagnoses of kidney transplant biopsies. *Transplantation*. 2022;106:1061–1070.
69. Xiao H, Gao F, Pang Q, et al. Diagnostic accuracy of donor-derived cell-free DNA in renal-allograft rejection: a meta-analysis. *Transplantation*. 2021;105:1303–1310.
70. Halloran PF. T cell-mediated rejection of kidney transplants: a personal viewpoint. *Am J Transplant*. 2010;10:1126–1134.
71. Furness PN, Taub N; Convergence of European Renal Transplant Pathology Assessment Procedures (CERTPAP) Project. International variation in the interpretation of renal transplant biopsies: report of the CERTPAP project. *Kidney Int*. 2001;60:1998–2012.